Quantitative retinal blood flow measurement with three-dimensional vessel geometry determination using ultrahigh-resolution Doppler optical coherence angiography

Shuichi Makita,* Tapio Fabritius, and Yoshiaki Yasuno

Computational Optics Group, University of Tsukuba,

1-1-1 Tenodai, Tsukuba, Ibaraki 305-8573, Japan

*Corresponding author: makita@optlab2.bk.tsukuba.ac.jp

Retinal blood flow quantification by retinal vessel segmentation with Doppler optical coherence angiography is presented. Vessel diameter, orientation, and position are determined in an *en face* vessel image and two representative cross-sectional flow images of the vessel. Absolute blood flow velocity is calculated with the help of measured Doppler frequency shift and determined vessel angle. The volumetric flow rate is obtained with the position and the region of the vessel lumen. The volumetric blood flow rate of retinal arteries before and after a bifurcation is verified in a healthy human eye. © 2008 Optical Society of America

Retinal blood flow measurement is required to determine the effect of hemodynamic abnormalities in retinal pathologies. There exist several blood flow measurement techniques that are applied to retinal vessels. Dye-dilution is a technique that involves tracing fluorescent dyes flowing in the retinal vessel by monitoring the fluorescence intensity. However, the dye injection is not comfortable for patients. Although laser Doppler velocimetry (LDV) can measure the volumetric flow rate of the retinal vessel [1], it requires dilation to collect two scattered beams with different scattering angles.

Doppler optical coherence tomography (Doppler OCT) is a technique used to observe cross-sectional flow images, and retinal blood flow distribution has been imaged. By using a spectral-domain detection technique, high-speed cross-sectional retinal blood flow imaging is achieved [2,3]. Furthermore, the three-dimensional (3D) retinal vasculature can be observed [4,5].

For obtaining the flow quantification with the Doppler OCT, several techniques have been developed, e.g., axial and transversal flow speeds measurement [6], and multi-angle detection techniques [7,8]. However, these techniques have several shortcomings for *in vivo* retinal blood flow measurement. For example, in order to measure the transversal velocity, a large number of samples are required. The multi-angle detection technique may requires dilation as LDV does. In addition, it results in the

limited axial range in spectral-domain OCT (SD-OCT). Recently, vessel segmentation techniques that calculate the vessel orientation are presented. Wang *et al.* [9] present total blood flow volume measurement with sampling all retinal arteries or veins around the optic nerve head. The vessel orientations are obtained from vectors connecting vessel centers between two successive cross section. In this technique, a straight portion of the vessel is aimed, and, these two cross sections should not be nearly parallel to the vessel. Full 3D processing is performed by Michaely *et al.* [10]. Although this method is comprehensive, it requires long computational time since an OCT volume set has a large number of voxels. In this letter, we demonstrate a retinal blood flow quantification with a two step computationally inexpensive retinal vessel segmentation with a two-dimensional (2D) *en face* retinal vessel image and 2D cross-sectional flow image.

For the absolute blood flow speed measurement with the Doppler OCT, the Doppler angle is required, and for the volumetric flow measurement, vessel lumen determination is needed. For that purpose, vessel segmentation is applied to determine the vessel parameters, i.e., the vessel orientation and diameter.

Since the retinal vasculature is distributed nearly parallel to the retinal surface, *en face* retinal vessel images illustrate the representative retinal vasculature. Thus, the vessel segmentation was performed in two steps. The 3D geometric parameters of the vessel are indicated in Fig. 1. The first step is the vessel azimuth θ, diameter D, and lateral position detection in the *en face* projection image E. The second step

is the vessel zenith ϕ and axial position detection in the cross-sectional vessel images (planes A and P). These vessel parameters are then used to determine the region of the vessel lumen S. This algorithm does not require processing for the entire 3D volume set; thus, the computational time is shortened.

The second derivatives of the $en\ face$ vessel image are used to determine the parameters of the curvilinear structure, namely, retinal vessels. For the segmentation of several sizes of vessels, a multi-scale technique [11] is used. The filtering operator is defined with second derivatives of a Gaussian function with a standard deviation σ, as $L = \left[\partial/\partial x, \partial/\partial y\right]^{T}\left[\partial/\partial x, \partial/\partial y\right] G(\mathbf{r}, \sigma)$. Applying this line filter to the vessel image I, we have a 2×2 matrix of the second derivatives of the image $\mathbf{H}(x, y) = L \otimes I(x, y)$. Vesselness F is calculated from the eigenvalues of the matrix $\mathbf{H}$, Λ_1 and Λ_2 $(\Lambda_1 > \Lambda_2)$, as follows: $F = \sqrt{|\Lambda_2|(|\Lambda_2| + \Lambda_1)}$ $(\Lambda_2 < \Lambda_1 \leq 0)$, $\sqrt{|\Lambda_2|(|\Lambda_2| - \alpha\Lambda_1)}$ $(\Lambda_2 < 0 < \Lambda_1 < \frac{|\Lambda_2|}{\alpha})$, or 0 (otherwise). These conditions are determined to discriminate a blob-like shape $(|\Lambda_1| \sim |\Lambda_2| \gg 0)$ from a curvilinear structure and make it sensitive to the discontinuity of the line structure $(\Lambda_2 < 0 < \Lambda_1)$. The value of α which determines the sensitivity to discontinuity is set to 0.25. Here, the vessels in the image are considered to possess a brighter intensity than that of the surroundings. Usually, retinal vessels cast shadows in $en\ face$ projection image of OCT volume set, so that inverted $en\ face$ image is used. The eigenvectors indicate the orientation of the line structure, namely, azimuth angle of the vessel, θ. For a multi-scale detection, this line filter is applied with several different deviations of the Gaussian function. Vesselness is then normalized

4

with the deviation of the Gaussian function σ as $\sigma F(\sigma)$. The vesselness at the applied point is defined as the maximum normalized vesselness $F' = \max[\sigma F(\sigma)]$, and the vessel diameter is defined as $D = 4\sigma_{\max}$, where $F' = \sigma_{\max}F(\sigma_{\max})$. The measured vessels are selected semi-automatically. The retinal vessels in the *en face* image are determined with a top-hat filter, followed by thresholding. Operator indicates a line cross over a retinal vessel. Then, the point along that line having the maximum vesselness is defined as the center of the vessel.

According to the azimuth angle θ and the central position of the vessel, a cross-sectional flow image (plane A in Fig. 1) line intersecting the vessel centerline is created from the 3D flow volume set. Line filtering with the standard deviation of the Gaussian function $\sigma_{\max}$ is applied to the unsigned flow image. The zenith angle (ϕ) of the vessel is corresponding to the line filter output at the center of the vessel. To determine the vessel position and the region of the vessel lumen, the depth of the vessel should be known. A cross-sectional bi-directional flow image intersecting the vessel (plane P in Fig. 1) is created from the 3D flow volume set. The correlation between this cross section and a circle with a diameter D is applied. The position of the maximum correlation point indicates the depth of the vessel. The zenith angle of the vessel can be considered as the Doppler angle when all the blood flow vectors are parallel.

With the help of the Doppler angle ϕ and Doppler frequency shift Δf, the blood flow velocity can be corrected, except the case $\phi \approx 90°$. Although this exceptional Doppler angle must be avoided in practice, it is not frequently occurred. The absolute blood

5

flow velocity V is obtained as $V = \lambda_0 \Delta f / (2n \cos \phi)$, where λ_0 is the central wavelength of the light source and n indicates the refractive index of the sample. According to the obtained vessel parameters, an elliptical vessel lumen S in the cross-sectional flow image (plane P) is estimated. The blood flow rate is obtained by the integration of the lateral blood flow velocity component, which is calculated from the Doppler frequency shift and the Doppler angle within the vessel lumen S as: $J = \sum_S \frac{\lambda_0 \Delta f}{2n} \tan \phi \Delta s$, where Δs is the area of one pixel in the cross-sectional flow image.

For the verification of this method, blood mass conservation is confirmed at a bifurcation of a retinal artery. The right eye of a healthy volunteer is scanned by an ultrahigh-resolution SD-OCT system [12] with 27.7 kHz of axial scan rate and ~ 3 μm of axial resolution in the tissue. 3D volume set with 196×28 axial scans (corresponding to 1 mm $\times$ 1 mm) is obtained within 225 ms. Since the voxel size is anisotropic, the segmentation accuracy and resulting measurement of blood flow will depend on the azimuth angle. Twenty volumes are scanned sequentially so that the total measurement time is 4.5 s. Since almost all the retinal vessels are nearly perpendicular to the incident beam, the Doppler frequency shifts can be relatively small. This results in a significant errors in the vessel segmentation algorithm. To avoid such a situation, an artery, rather than a vein, is used since the Doppler frequency shift of the arteries is larger than that of the veins. For Doppler shift flow imaging, the Kasai correlator is applied to the complex OCT image.To avoid a 2π-phase ambiguity in the flow image, which causes the limited Doppler frequency range, a 2D phase

unwrapping algorithm [13] is applied to a portion of the flow image wherein the phase wrapping has occurred. Motion artifacts of the flow images are removed by a histogram-based method, and image distortion due to the bulk motion is numerically corrected [4]. To obtain a high-contrast *en face* retinal vessel image, the maximum log-intensity projection of the 3D retinal OCT volume set just around the retinal pigment epithelium (RPE) is calculated (Fig. 3 B).

The multi-scale line filtering results of one measurement are shown in Fig. 2. Accordingly, the vessel segmentation is performed and results are shown in Fig. 3. The computational time of the vessel segmentation and flow calculation for each volume (3 vessels) are $\sim$ 3 min with a PC (AMD Athlon 64 3500+, 2 GB RAM). An semi-automatic registration of the *en face* image and a fundus photograph (Fig. 3 A) is performed, and the area corresponding to the scanning region is indicated as the white box. The red lines in Fig. 3 B indicate the cross-sectional planes parallel to the retinal vessels, and the blue lines are the perpendicular cross sections. At the vessel 2, the azimuth angle have the small tilt although the vessel seems to be nearly horizontal. However, the corresponding fundus photography (Fig. 3 A) shows the slight azimuth angle of vessel 2. It can be considered that the multi-scale line filtering is sensitive to the sub-pixel ordered structure. The cross-sectional flow images parallel and perpendicular to the retinal vessel are shown in Figs. 3 C–H. These images are consisting of nearest voxels from the 3D flow volume set according to *en face* positions. The determined vessel boundaries are indicated with ellipses in Figs. 3 C, E, and G. The

red lines in Figs. 3 D, F, and H are the tangential lines to the centerline of the vessels at the center of the images.

The blood flow parameters are obtained for all of the 20 volume sets and the mean of the peak velocity V_{peak}, diameter D, and volumetric flow rate J are shown in Table1. The signs of the blood flow velocity and flow rate indicate the direction of flow — incoming to $(+)$ or outgoing from $(-)$ the bifurcation. The plot of volumetric flow rate of vessel 1 versus total flow rate of vessels 2 and 3 is shown in Fig. 4. The measured incoming and outgoing blood volumes are in direct proportion. The intraclass correlation coefficient is 0.74. The mean of the total outgoing blood flow rate, 3.41 μl/min, is comparable to the incoming blood flow rate, 3.23 μl/min. Since the blood flow in the arteries are measured, the standard deviations of the blood flow rates are relatively large as compared to the mean flow rates due to pulsation.

In conclusion, the vessel parameters—orientation and diameter—are determined with a two-step 2D image-based processing method. The retinal blood flow velocity and volumetric flow rate are quantitatively obtained. To the best of our knowledge, this is the first study of conservation of blood flow at a bifurcation of the retinal artery with a cross-sectional flow imaging technique.

ogy Agency, and the Special Research Project of Nanoscience at the University of Tsukuba. Shuichi Makita is a JSPS research fellow.

References

1. C. E. Riva, J. E. Grunwald, S. H. Sinclair, and B. L. Petrig, Invest. Ophthalmol. Vis. Sci. **26**, 1124 (1985).

2. R. Leitgeb, L. Schmetterer, W. Drexler, A. Fercher, R. Zawadzki, and T. Bajraszewski, Opt. Express **11**, 3116 (2003).

3. B. R. White, M. C. Pierce, N. Nassif, B. Cense, B. H. Park, G. J. Tearney, B. E. Bouma, T. C. Chen, and J. F. de Boer, Opt. Express **11**, 3490 (2003).

4. S. Makita, Y. Hong, M. Yamanari, T. Yatagai, and Y. Yasuno, Opt. Express **14**, 7821 (2006).

5. A. H. Bachmann, M. L. Villiger, C. Blatter, T. Lasser, and R. A. Leitgeb, Opt. Express **15**, 408 (2007).

6. D. Piao and Q. Zhu, Appl. Opt. **42**, 5158 (2003).

7. C. J. Pedersen, D. Huang, M. A. Shure, and A. M. Rollins, Opt. Lett. **32**, 506 (2007).

8. Y. C. Ahn, W. Jung, and Z. Chen, Opt. Lett. **32**, 1587 (2007).

9. Y. Wang, B. A. Bower, J. A. Izatt, O. Tan, and D. Huang, J. Biomed. Opt. **12**, 041215 (2007).

10. R. Michaely, A. H. Bachmann, M. L. Villiger, C. Blatter, T. Lasser, and R. A.

Leitgeb, J. Biomed. Opt. **12**, 041213 (2007).

11. T. Koller, G. Gerig, G. Szekely, and D. Dettwiler, in *Proceedings of the Fifth International Conference on Computer Vision* (IEEE, 1995), pp. 864–869.

12. Y. Hong, S. Makita, M. Yamanari, M. Miura, S. Kim, T. Yatagai, and Y. Yasuno, Opt. Express **15**, 7538 (2007).

13. D. Ghiglia and L. Romero, J. Opt. Soc. Am. A **11**, 107 (1994).

References

1. C. E. Riva, J. E. Grunwald, S. H. Sinclair, and B. L. Petrig, "Blood velocity and volumetric flow rate in human retinal vessels." Invest. Ophthalmol. Vis. Sci. **26**, 1124–1132 (1985).

2. R. Leitgeb, L. Schmetterer, W. Drexler, A. Fercher, R. Zawadzki, and T. Bajraszewski, "Real-time assessment of retinal blood flow with ultrafast acquisition by color Doppler Fourier domain optical coherence tomography," Opt. Express **11**, 3116–3121 (2003).

3. B. R. White, M. C. Pierce, N. Nassif, B. Cense, B. H. Park, G. J. Tearney, B. E. Bouma, T. C. Chen, and J. F. de Boer, "In vivo dynamic human retinal blood flow imaging using ultra-high-speed spectral domain optical Doppler tomography," Opt. Express **11**, 3490–3497 (2003).

4. S. Makita, Y. Hong, M. Yamanari, T. Yatagai, and Y. Yasuno, "Optical coherence angiography," Opt. Express **14**, 7821–7840 (2006).

5. A. H. Bachmann, M. L. Villiger, C. Blatter, T. Lasser, and R. A. Leitgeb, "Resonant Doppler flow imaging and optical vivisection of retinal blood vessels," Opt. Express **15**, 408–422 (2007).

6. D. Piao and Q. Zhu, "Quantifying Doppler angle and mapping flow velocity by a combination of Doppler-shift and Doppler-bandwidth measurements in optical

Doppler tomography," Appl. Opt. **42**, 5158–5166 (2003).

7. C. J. Pedersen, D. Huang, M. A. Shure, and A. M. Rollins, "Measurement of absolute flow velocity vector using dual-angle, delay-encoded Doppler optical coherence tomography," Opt. Lett. **32**, 506–508 (2007).

8. Y. C. Ahn, W. Jung, and Z. Chen, "Quantification of a three-dimensional velocity vector using spectral-domain Doppler optical coherence tomography," Opt. Lett. **32**, 1587–1589 (2007).

9. Y. Wang, B. A. Bower, J. A. Izatt, O. Tan, and D. Huang, "In vivo total retinal blood flow measurement by Fourier domain Doppler optical coherence tomography," J. Biomed. Opt. **12**, 041215 (2007).

10. R. Michaely, A. H. Bachmann, M. L. Villiger, C. Blatter, T. Lasser, and R. A. Leitgeb, "Vectorial reconstruction of retinal blood flow in three dimensions measured with high resolution resonant Doppler Fourier domain optical coherence tomography," J. Biomed. Opt. **12**, 041213 (2007).

11. T. Koller, G. Gerig, G. Szekely, and D. Dettwiler, "Multiscale detection of curvilinear structures in 2-d and 3-d image data," in "Proceedings of the Fifth International Conference on Computer Vision," (IEEE, 1995), pp. 864–869.

12. Y. Hong, S. Makita, M. Yamanari, M. Miura, S. Kim, T. Yatagai, and Y. Yasuno, "Three-dimensional visualization of choroidal vessels by using standard

and ultra-high resolution scattering optical coherence angiography," Opt. Express **15**, 7538–7550 (2007).

13. D. Ghiglia and L. Romero, "Robust two-dimensional weighted and unweighted phase unwrapping that uses fast transforms and iterative methods," J. Opt. Soc. Am. A **11**, 107–117 (1994).

Table 1. Blood flow measurement results.

	V_{peak} [mm/s]	D [μm]	J [μl/min]
1	+ 22.5	137	+ 3.23 ± 1.3
2	- 17.4	52.4	- 1.09 ± 0.83
3	- 30.2	71.0	- 2.32 ± 1.1

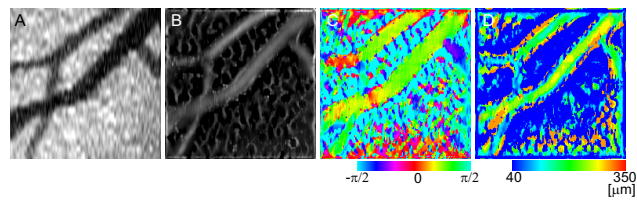**List of Figures**

Fig. 1. Schematic diagram of vessel geometry.

Fig. 2. Multi-scale line filtering results. From the *en face* vessel image (A), the distributions of the vesselness (B), azimuth (C), and diameter (D) are obtained.
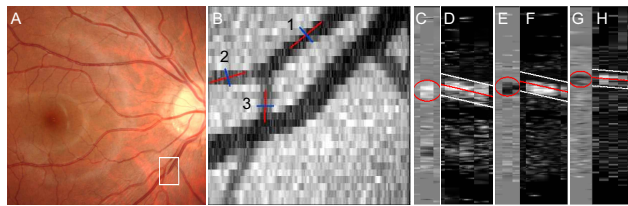
Fig. 3. Vessel segmentation results for a bifurcation of a retinal artery. C,E,G: Cross-sectional flow images of each vessel in the P-plane; D,F,H: those in the A-plane.
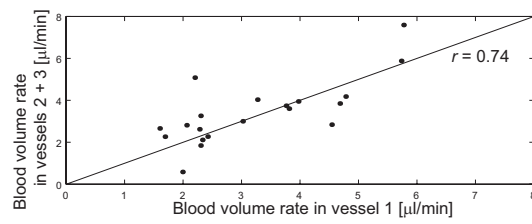
Fig. 4. The relationship of measured blood flow volume rate before and after the bifurcation at different time during the heat beat.